Charge transmission through a molecular wire: The role of terminal sites for the current-voltage behavior

E. G. Petrov and Ya. R. Zelinskyy
Bogolyubov Institute for Theoretical Physics, National Academy of Sciences of Ukraine, Metrologichna strasse 14-b, UA-03143 Kiev, Ukraine

V. May
Institut für Physik, Humboldt Universität zu Berlin, Newtonstrasse 15, D-12489 Berlin, Germany

P. Hänggi
Institut für Physik, Universität Augsburg, Universitätsstrasse 1, D-86135 Augsburg, Germany

(Received 10 July 2006; accepted 11 July 2007; published online 31 August 2007)

The current-voltage and the conductance-voltage characteristics are analyzed for a particular type of molecular wire embedded between two electrodes. The wire is characterized by internal molecular units where the lowest occupied molecular orbital (LUMO) levels are positioned much above the Fermi energy of the electrodes, as well as above the LUMO levels of the terminal wire units. The latter act as specific intermediate donor and acceptor sites which in turn control the current formation via the superexchange and sequential electron transfer mechanisms. According to the chosen wire structure, intramolecular multiphonon processes may block the superexchange component of the interelectrode current, resulting in a *negative differential resistance* of the molecular wire. A pronounced current *rectification* appears if (i) the superexchange component dominates the electron transfer between the terminal sites and if (ii) the multiphonon suppression of distant superexchange charge hopping events between those sites is nonsymmetric. © *2007 American Institute of Physics*. [DOI: 10.1063/1.2768521]

I. INTRODUCTION

The progress achieved during the past decades in applying scanning probe techniques, as well as the break junction methods, facilitated current measurements through single molecules. They could be demonstrated to operate as molecular switches,[1,2] diodes,[3–5,7] transistors,[6–9] sensors,[10] memory storage devices,[11,12] etc. The current through a single molecule is controlled by a whole set of different factors: the electronic structure of the molecule, the type of molecule-electrode coupling, and the position of the lowest unoccupied/highest occupied molecular orbitals (LUMO/HOMOs) with respect to the Fermi levels of each electrode, to name a few.[13–15] Electronic structure calculations shed valuable light on the electronic spectrum, the charge distribution, and the density of states of the molecule-electrodes system.[16–23]

An important theoretical tool for computing the current through a single molecule is given by the Landauer theory, originally developed in mesoscopic physics.[24,25] Its applicability to the description of charge transmission through a single molecule embedded in between two electrodes, however, is rather restricted, even though some recent modifications also account for molecular vibrational degrees of freedom.[26–35] The restricted practicability is caused by the fact that the Landauer theory only describes the direct (tunnel) route of interelectrode charge transfer.

Meanwhile, the so-called sequential route has been also considered, accounting for relaxation processes in the course of charge transmission through the molecule or the molecular wire.[36–41] A comprehensive description of charge transmission becomes possible either in the framework of the nonequilibrium Green's function (NGF) technique or by use of a corresponding density matrix theory. Using the first technique, particular self-energy expressions may be introduced to account for the different types of vibrational coupling to the charge transmission process through the molecule.[8,27,35,42–45] Charge transmission including multiples of vibrational quanta (multiphonon processes), however, can advantageously be considered when using the density matrix method. Such an approach has been already utilized by the authors before to achieve a unified description of bridge-mediated donor-acceptor electron transfer [46–49] (ET) as well as electron transmission through single molecules and molecular wires.[41,50–54]

The NGF method combined with density functional theory offers a atomic structure based approach for computing the conductance of single molecules and molecular wires. So far, however, there remain numerous effects which can only be accounted for in the framework of a semiphenomenological description, for example, the coupling of molecular degrees of freedom to a dissipative environment. In this spirit, the present work utilizes the density matrix method to elucidate how terminal groups of a molecular wire may dominate its current-voltage (*I-V*) characteristics. Towards this goal, we will consider a model of a molecular wire which consists of a terminal donor and acceptor group as well as of an internal molecular bridge. Such a system has been already investigated earlier in Refs. 36, 55, and 56 however, exclusively concentrating on the superexchange elec-

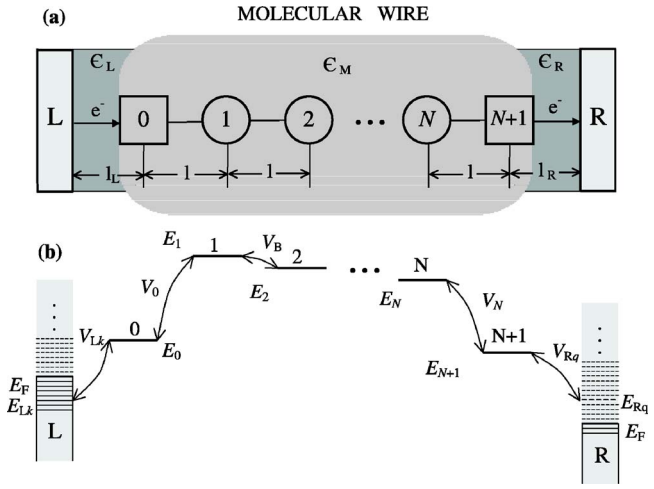

FIG. 1. Left electrode-molecular wire-right electrode system (panel a) and the related energy level scheme (panel b). The electron affinities $E_1, E_2, \ldots, E_N$, Eq. (5), of the internal wire units are smaller than the affinities E_0 and E_{N+1} related to the terminal units. Therefore, the latter can be considered as the donor and the acceptor site, respectively, connected by the bridge of internal wire units.

tron pathway between the terminal groups (cf. Ref. 36). It was possible to explain the relation between the differential resistance and the superexchange donor-acceptor transfer rate.[55] The influence of the donor-acceptor superexchange interaction on the *I-V* characteristics has been studied in Ref. 56.

In contrast to these studies we will investigate the nonadiabatic ET regime. It will be demonstrated that the current formation strongly depends on the relation between the *contact transfer rates* (electron hopping between the electrodes and the adjacent terminal sites of the wire) and the overall transfer rate characterizing the distant single step ET between the terminal sites. The overall transfer rate includes superexchange as well as sequential contributions. We will analyze in detail the transmission regimes characterized by large and small contact transfer rates (weak and strong coupling cases, respectively). Here, it has been found that for a weak coupling (when the limiting step of transmission is caused by the contact transfer rates), a rectification effect is not significant even at the resonant regime of transmission. At a strong coupling to the electrodes, however, the molecular wire may act as a rectifier. This is due to the fact that the limiting step of ET, now, is determined by the distant hopping between the terminal sites. If the distant hopping is mainly determined by the superexchange coupling between the terminal sites, then the rectification strongly depends on the relation between the voltage switches at resonant transmission and the voltages at which the overall transfer rates achieve their maximum.

II. MODEL AND BASIC EXPRESSION FOR THE CURRENT

ET through a molecular wire, cf. Fig. 1(a), is of the nonadiabatic type if the characteristic time τ_{hop} of electron jumps between different sites of electron localization is much larger than the intrasite vibrational relaxation time τ_{rel}, i.e.,

$$\tau_{\mathrm{hop}} \gg \tau_{\mathrm{rel}}. \tag{1}$$

In such a case, the ET proceeds against the background of fast relaxation processes, and it is thus most appropriate to describe ET in the "left electrode-molecular wire-right electrode" (*L*-MW-*R*) system in using the basis of localized molecular electron-vibrational states. This tight-binding-type description of the molecular wire should at least comprise a single electronic level and a single active vibrational coordinate per site.

A. Hamiltonian of the *L*-MW-*R* system

Denoting the vibrational levels of the nth site by ν_n and introducing the notation $|n\nu_n\rangle$ as the respective electron-vibrational state, the wire Hamiltonian takes the following form:

$$H_W = \sum_{n=0}^{N+1} \Bigg[\sum_{\nu_n} \varepsilon_{n\nu_n} |n\nu_n\rangle\langle n\nu_n| + \sum_{\nu_n,\nu_{n+1}} \sum_{\nu_n^{(0)},\nu_{n+1}^{(0)}} ((1-\delta_{n,N+1}) V_{\nu_n \nu_{n+1}^{(0)},\nu_n^{(0)}\nu_{n+1}} \times |n\nu_n\rangle|n+1\,\nu_{n+1}^{(0)}\rangle\langle n\nu_n^{(0)}|\langle n+1\,\nu_{n+1}| + \mathrm{H.c.}) \Bigg]. \tag{2}$$

The expression contains the transfer coupling $V_{\nu_n \nu_{n+1}^{(0)},\nu_n^{(0)}\nu_{n+1}}$, which is responsible for electron transitions between the electron-vibrational states of the neighboring sites $n+1$ and n. Moreover, the $|n\nu_n^{(0)}\rangle$ are the electron-vibrational states of site n at the absence of the transferred electron (empty site). Note here the use of the superscript 0 to indicate the states related to the empty sites. The energy of the $n\nu_n$-th electron-vibrational state (at the presence of the transferred electron) reads

$$\varepsilon_{n\nu_n} = \varepsilon_n + \hbar\omega_n(1/2 + \nu_n). \tag{3}$$

The energy ε_n is defined by the minimum of the respective potential energy surface, and ω_n is the corresponding vibrational frequency. The electron-vibrational energies of site n at the absence of the transferred electron are denoted as

$$\varepsilon_{n\nu_n^{(0)}}^{(0)} = \varepsilon_n^{(0)} + \hbar\omega_n(1/2 + \nu_n^{(0)}). \tag{4}$$

Consequently, the difference

$$E_n = \varepsilon_n - \varepsilon_n^{(0)} \tag{5}$$

gives the electron affinity of site n (note our use of the Holstein's model[57] where the vibrational frequencies ω_n are independent on the charging of the site).

The electronic states which belong to the conduction band of the electrode $s=L,R$ are denoted as $|s\mathbf{k}\sigma\rangle$ with the electronic quasi-wave-vector $\mathbf{k}$ and the spin quantum number σ. Since we focus on transitions between nonmagnetic electrodes at the absence of a magnetic field, the single-electron energy $E_{s\mathbf{k}}$ becomes independent on σ. Therefore, the electronic Hamiltonian of the sth electrode reads

$$H_s = \sum_{\mathbf{k}\sigma} E_{s\mathbf{k}} |s\mathbf{k}\sigma\rangle\langle s\mathbf{k}\sigma| \quad (s = L,R), \tag{6}$$

and the coupling of the sth electrode with the molecular wire can be written as

$$V_{sW} = \sum_{n\mathbf{k}\sigma} \sum_{\nu_n \nu_n^{(0)}} [V_{s\mathbf{k}\nu_n^{(0)},n\nu_n}(\delta_{s,L}\delta_{n,0} + \delta_{s,R}\delta_{n,N+1})|s\mathbf{k}\sigma\rangle \times |n\nu_n^{(0)}\rangle\langle n\nu_n| + \text{H.c.}]. \tag{7}$$

Transitions from the state $|n\nu_n\rangle$ to a band state $|s\mathbf{k}\rangle$ of the sth electrode and the $\nu_n^{(0)}$-th vibrational state of the empty site n are characterized by the transfer matrix element $V_{s\mathbf{k}\nu_n^{(0)},n\nu_n}$. In what follows, we apply the Condon approximation to obtain

$$V_{\nu_n \nu_{n+1}^{(0)},\nu_n^{(0)}\nu_{n+1}} \approx V_n \langle \nu_{n+1}^{(0)}|\nu_{n+1}\rangle\langle \nu_n|\nu_n^{(0)}\rangle,$$
$$V_{s\mathbf{k}\nu_n^{(0)}n\nu_n} \approx V_{s\mathbf{k}} \langle \nu_n^{(0)}|\nu_n\rangle. \tag{8}$$

Here, V_n is the electronic transfer coupling between the molecular orbitals (MOs) of the internal wire site n and $n+1$, while $V_{s\mathbf{k}}$ describes the coupling between the $\mathbf{k}$th conduction band state of electrode s and the MO of the opposite terminal wire site [cf. Fig. 1(b)]. $\langle \nu_n^{(0)}|\nu_n\rangle$ denotes the overlap integral between the vibrational wave functions of the empty and the singly charged state of site n. The expressions (2), (6), and (7), determine the desirable electron-vibrational Hamiltonian of the L-MW-R system,

$$H = \sum_{s=L,R} (H_s + H_{sW}) + H_W. \tag{9}$$

B. Hopping current at negligible bridge population

In order to derive an analytic expression for the current through a molecular wire, we start out from the general current formula,

$$I(t) = -e\sum_{\sigma} \dot{N}_{L\sigma}(t), \tag{10}$$

where $e>0$ denotes the absolute value of electron charge, and $\dot{N}_{L\sigma}(t) = \Sigma_{\mathbf{k}} \dot{P}_{L\mathbf{k}\sigma}(t)$ is the time derivative of the total number of electrons in the left electrode with spin σ. The quantity $\Sigma_\sigma \dot{N}_{L\sigma}(t) = -\Sigma_\sigma \dot{N}_{R\sigma}(t)$ is associated with a net interelectrode charge flow. The latter appears as a kinetic process in the L-MW-R system and includes long-range tunnel and short-range sequential charge hoppings. There exists a unified description of such complicated kinetic processes.[41,52,53] The considerations following hereafter are based on this method. In using the Hamiltonian, Eq. (9), we are able to derive nonlinear kinetic equations for the electrode conduction band populations $P_{L\mathbf{k}\sigma}(t)$ and thus for the charge flow $\Sigma_\sigma \dot{N}_{L\sigma}(t)$. In what follows, the conductive band is considered in the so-called wideband limit. This simplification allows one to reduce the emerging nonlinear equations for the $P_{L\mathbf{k}\sigma}(t)$ to linear ones (for more details we refer the readers to Ref. 50). Note, however, that the precise form of these equations depends on the strength of Coulomb interaction within the L-MW-R system. Here, we restrict ourself to the case of a strong Coulomb interaction between the transferred

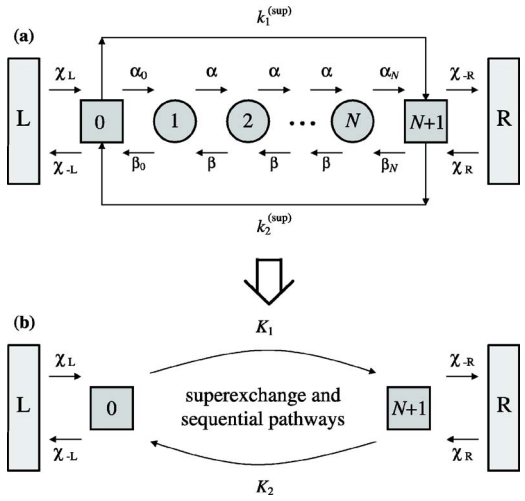

FIG. 2. Kinetic schemes of electron transmission through a molecular wire. If the population of the internal wire sites $1,2,\ldots,N$ is small a complete hopping process in the L-MW-R system (panel a) can be reduced to a much more simple hopping process with the participation of the terminal sites 0 and $N+1$ only. In the reduced scheme (panel b), the hopping transition between terminal sites is characterized by the overall transfer rates K_1 and K_2, including sequential and superexchange contributions.

electrons occupying the wire in the course of transmission. In our context this means that in a given voltage region only a single extra electron can be captured by the wire. For such a single-electron transfer the following normalization condition has to be satisfied for the wire state populations:

$$\mathcal{P}_{\text{empty}}(t) + \sum_{n=0}^{N+1} \sum_{\sigma} \mathcal{P}_{n\sigma}(t) = 1. \tag{11}$$

The population $\mathcal{P}_{\text{empty}}(t)$ matches the probability to find the wire without an extra (transferred) electron. In contrast, the population $\mathcal{P}_{n\sigma}(t)$ gives the probability that the wire unit n contains a single extra electron (with spin projection σ) whereas other wire units are free from extra electrons. With the introduction of the wire populations we may derive

$$\dot{N}_{L\sigma}(t) = -\chi_L \mathcal{P}_{\text{empty}}(t) + \chi_{-L}\mathcal{P}_{1\sigma}(t). \tag{12}$$

The contact transfer rates χ_L and χ_{-L} characterize the electron hopping between the terminal unit 0 and the adjacent electrode L, cf. Fig. 2(a). Analogously, one introduces the contact transfer rates χ_R and χ_{-R} characterizing an electron hopping between the terminal unit $N+1$ and the adjacent electrode R. Based on the unified description of ET processes we can also derive the kinetic equations for the wire populations $\mathcal{P}_{n\sigma}(t)$, $(n=0,1,\ldots,N+1)$, and, additionally, all characteristic hopping rates indicated in the scheme of Fig. 2(a). The rate constants $k_1^{(sup)} \equiv k_{0N+1}$ and $k_2^{(sup)} \equiv k_{N+10}$ characterize the distant electron hopping between the terminal units 0 and $N+1$, while the rate constants $\alpha_0 \equiv k_{01}$, $\alpha \equiv k_{nn+1}$, $\alpha_N \equiv k_{NN+1}$, $\beta_0 \equiv k_{10}$, $\beta \equiv k_{NN+1}$, and $\beta_N \equiv k_{N+1N}$ describe hopping transitions between neighboring units.

We next concentrate on such a transfer regime at which the population of any internal wire unit remains negligibly small during the charge transmission. Consequently, this bridge-assisted transmission regime is met if

$$\mathcal{P}_{n\sigma}(t) \ll 1 \quad (n=1,2,\ldots,N). \tag{13}$$

The necessary and sufficient conditions to reach such a regime has been formulated in prior work (see Ref. 47). In the present notation, these conditions imply the inequalities

$$\beta_0 \gg (N/2)\alpha_0, \quad \alpha_N \gg (N/2)\beta_N. \tag{14}$$

If these inequalities, as well as the inequality (13), are fulfilled, the kinetics of nonadiabatic charge transfer within the L-MW-R system [cf. Fig. 2(a)] is reduced to a more simple transfer process depicted in Fig. 2(b). In this regime, the set of $N+3$ kinetic equations for all wire populations is reduced to the set of equations for only three populations, reading

$$\dot{\mathcal{P}}_{\text{empty}}(t) = -2(\chi_L+\chi_R)\mathcal{P}_{\text{empty}}(t) + \sum_\sigma \chi_{-L}\mathcal{P}_{0\sigma}(t) + \sum_\sigma \chi_{-R}\mathcal{P}_{N+1\sigma}(t),$$

$$\dot{\mathcal{P}}_{0\sigma}(t) = -(\chi_{-L}+K_1)\mathcal{P}_{0\sigma}(t) + \chi_L\mathcal{P}_{\text{empty}}(t) + K_2\mathcal{P}_{N+1\sigma}(t), \tag{15}$$

$$\dot{\mathcal{P}}_{N+1\sigma}(t) = -(\chi_{-R}+K_2)\mathcal{P}_{N+1\sigma}(t) + \chi_R\mathcal{P}_{\text{empty}}(t) + K_1\mathcal{P}_{0\sigma}(t).$$

In line with Eqs. (11) and (13) these equations are coupled by a simple normalization condition,

$$\mathcal{P}_{\text{empty}}(t) + \sum_\sigma [\mathcal{P}_{0\sigma}(t) + \mathcal{P}_{N+1\sigma}(t)] \simeq 1. \tag{16}$$

Note the appearance of the overall transfer rates K_1 and K_2, which, in fact, include the superexchange and the sequential contributions,[58]

$$K_{1(2)} = k_{1(2)}^{(\text{sup})} + k_{1(2)}^{(\text{seq})}. \tag{17}$$

Here, the superexchange rate constants $k_1^{(\text{sup})}$ and $k_2^{(\text{sup})}$ describe single step electron jumps between the terminal wire units. They decrease exponentially with increasing wire length, see below. The sequential rate constants $k_1^{(\text{seq})}$ and $k_2^{(\text{seq})}$ include the electron jumps between the neighboring wire units. For a wire with a regular spatial arrangement of its internal units, one finds

$$k_1^{(\text{seq})} = \alpha_0\alpha^{N-1}\alpha_N/S, \quad k_2^{(\text{seq})} = \beta_0\beta^{N-1}\beta_N/S, \tag{18}$$

where

$$S = \alpha_N\alpha^{N-1} + \beta\beta^{N-1} + \alpha_N\beta_0\phi(N-2), \tag{19}$$

and

$$\phi(M) \equiv (\alpha\beta)^{M/2}\frac{\sinh[\kappa(M+1)]}{\sinh\kappa} \quad (e^\kappa = \sqrt{\alpha/\beta}). \tag{20}$$

Since we are exclusively interested in a description of the stationary transmission regime, the set of kinetic equations [Eq. (15)] is solved for $\dot{\mathcal{P}}_{\text{empty}}(t)=0$ and $\dot{\mathcal{P}}_{0\sigma}(t)=\dot{\mathcal{P}}_{N+1\sigma}(t)=0$. With the use of the normalization condition (16), we obtain

$$\mathcal{P}_{\text{empty}} = [\chi_L\chi_R + \chi_{-L}K_1 + \chi_{-R}K_2]/D,$$

$$\mathcal{P}_0 \equiv \mathcal{P}_{0\uparrow} = \mathcal{P}_{0\downarrow} = [\chi_L\chi_{-R} + (\chi_L+\chi_R)K_2]/D, \tag{21}$$

$$\mathcal{P}_{N+1} \equiv \mathcal{P}_{N+1\uparrow} = \mathcal{P}_{N+1\downarrow} = [\chi_L\chi_{-L} + (\chi_L+\chi_R)K_1]/D,$$

where

$$D = \chi_L\chi_R + \chi_{-L}(2\chi_R+K_2) + \chi_{-R}(2\chi_L+K_1) + 2(\chi_L+\chi_R)(K_1+K_2). \tag{22}$$

Now, based on Eqs. (10) and (12), one can derive an analytic expression for the stationary current,

$$I = I_0 2\pi\hbar(\chi_L\mathcal{P}_{\text{empty}} - \chi_{-L}\mathcal{P}_0), \tag{23}$$

or in an equivalent form,

$$I = -I_0 2\pi\hbar(\chi_R\mathcal{P}_{\text{empty}} - \chi_{-R}\mathcal{P}_{N+1}). \tag{24}$$

Note here the introduction of the quantity $I_0 \equiv (e/\pi\hbar) \times 1\ \text{eV} \approx 77.5\ \mu\text{A}$. The form of the current expression given in Eq. (23) is more suitable to describe the current formation at $V \geqslant 0$. Likewise, the preferable form is Eq. (24) if one analyzes the I-V characteristics at $V \leqslant 0$.

C. Transfer rates and rate constants

1. Transfer rates

In the case of the tight-binding model where the L-MW-R Hamiltonian is specified by Eq. (9), we find the following expression for a contact electrode-wire transfer rate:

$$\chi_s = \frac{1}{\hbar}\int_{-\infty}^{+\infty} dE\Gamma_s(E)f_s(E-\mu_s)(\text{FC})_{s\to n}(E). \tag{25}$$

Note that $n=0$ if $s=L$, and $n=N+1$ if $s=R$. In Eq. (25), $\Gamma_s(E)=2\pi\Sigma_{\mathbf{k}}|V_{s\mathbf{k}}|^2\delta(E-E_{s\mathbf{k}})$ defines the width parameter that determines the broadening $(\Gamma_s/2)$ of the level belonging to the terminal site adjacent to the sth electrode, and $f_s(E-\mu_s)$ denotes the Fermi distribution for the corresponding electrode with μ_s being the chemical potential. $(\text{FC})_{s\to n}(E) = \Sigma_{\nu_n,\nu_n^{(0)}}\langle\nu_n|\nu_n^{(0)}\rangle^2 W(\nu_n^{(0)})\delta(E-E_n-\hbar\omega_n(\nu_n-\nu_n^{(0)}))$ is the Franck-Condon factor associated with electron transition from the s electrode to the respective terminal site. It contains an equilibrium distribution function with respect to the electron-vibrational states of the uncharged site n, $W(\nu_n^{(0)}) = \exp(-\hbar\omega_n\nu_n^{(0)}/k_BT)/\Sigma_{\nu_n^{(0)}}\exp(-\hbar\omega_n\nu_n^{(0)}/k_BT)$. The expression for the contact wire-electrode transfer rate χ_{-s} follows from Eq. (25). Here, one only has to replace $f_s(E-\mu_s)$ by $1-f_s(E-\mu_s)$ and the Franck-Condon factor $(\text{FC})_{s\to n}(E)$ by $(\text{FC})_{n\to s}(E)$, related to an electron transition from the n-th terminal site to the adjacent electrode s. The difference between the $(\text{FC})_{s\to n}(E)$ and $(\text{FC})_{n\to s}(E)$ is caused by the electron-vibrational distribution function. The $(\text{FC})_{n\to s}(E)$ are defined by the $W(\nu_n)$.

An analytic calculation of the contact transfer rates χ_s and χ_{-s} is rather complicated, but can be performed for a concrete model of a thermal bath. One expression suitable for further analysis can be taken from Ref. 53. The corresponding derivation is based on the wideband approxima-

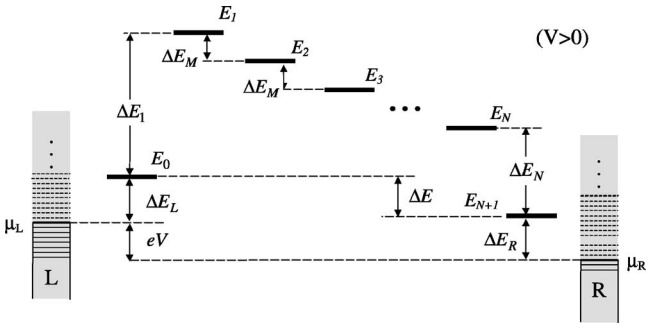

FIG. 3. Energy gaps according to Eqs. (29)–(37) for a regular molecular wire with two terminal and N internal units ($\mu_L=E_F$ and $\mu_R=E_F-eV$).

tion, at which the width parameter Γ_s displays a negligible dependence on the transmission energy E. Using this same approximation, one finds

$$\chi_{-s}=e^{\Delta E_s/k_BT}\chi_s, \quad \chi_s=\frac{1}{\hbar}\Gamma_s F_s, \tag{26}$$

where we have introduced the vibrational factor

$$F_s=2\pi\sum_{\nu_n,\nu_n^{(0)}}\langle\nu_n|\nu_n^{(0)}\rangle^2 W(\nu_n^{(0)})n_F(\Delta E_s+\hbar\omega_n(\nu_n-\nu_n^{(0)})), \tag{27}$$

with

$$n_F(\Delta E_s+\hbar\omega_n(\nu_n-\nu_n^{(0)}))=\frac{1}{\exp[\Delta E_s+\hbar\omega_n(\nu_n-\nu_n^{(0)}))/k_BT]+1} \tag{28}$$

being the particular distribution function. In Eqs. (26) and (28), the energy gaps between the terminal site levels and the respective Fermi levels of the electrodes are defined as

$$\Delta E_L=E_0-\mu_L=\Delta E_L(0)-eV\eta_L,$$
$$\Delta E_R=E_{N+1}-\mu_R=\Delta E_R(0)+eV\eta_R. \tag{29}$$

For the sake of definiteness, we suppose that the left electrode is grounded in such a manner that $\mu_L=E_F$ and $\mu_R=E_F-eV$. In Eq. (29), $\Delta E_L(0)=E_0(0)-E_F$ and $\Delta E_R(0)=E_{N+1}(0)-E_F$ are the respective unbiased gaps [for identical terminal units we have $E_{N+1}(0)=E_0(0)$ and thus $\Delta E_R(0)=\Delta E_L(0)$]. At a small rearrangement of the nuclear equilibrium configurations upon a recharging of the terminal groups, one may set $\langle\nu_n|\nu_n^{(0)}\rangle\approx\delta_{\nu_n,\nu_n^{(0)}}$. This approximation reduces the vibration factor, Eq. (27), to the simple form $F_s\approx 2\pi n_F(\Delta E_s)$ and, therefore,

$$\chi_{L(R)}=\frac{1}{\hbar}\Gamma_{L(R)}n_F(\Delta E_{L(R)}),$$
$$\chi_{-L(-R)}=\frac{1}{\hbar}\Gamma_{L(R)}[1-n_F(\Delta E_{L(R)})]. \tag{30}$$

These simplified forms of the contact transfer rates, Eq. (30), contain distribution functions with the electronic gaps [Eq. (29)]. The latter are depicted with Fig. 3.

2. Site-to-site rate constants

Apart from site-to-electrode electronic gaps [Eq. (29)] there exist site-to-site electronic energy gaps [cf. Eq. (29)]. They are defined by the relations, cf. also Fig. 3,

$$\Delta E_1=E_1-E_0=\Delta E_1(0)-eV\eta_M,$$
$$\Delta E_M=E_n-E_{n+1}=eV\eta_M \quad (n=1,\ldots,N), \tag{31}$$
$$\Delta E_N=E_N-E_{N+1}=\Delta E_N(0)+eV\eta_M.$$

These gaps refer to the levels belonging the neighboring wire sites. Here, $\Delta E_1(0)\equiv E_1(0)-E_0(0)$ and $\Delta E_N(0)\equiv E_N(0)-E_{N+1}(0)$ denote the unbiased intersite gaps [notably, for a regular wire and identical terminal units, we have $E_1(0)=E_N(0)$ and thus $\Delta E_N(0)=\Delta E_1(0)$]. In Eqs. (29) and (31), the parameters $\eta_L\equiv\delta_L/\delta$, $\eta_R\equiv\delta_R/\delta$, and $\eta_M\equiv\delta_M/\delta$ define the voltage induced shift of each level. These parameters are determined by the quantities $\delta\equiv\delta_L+(N+1)\delta_M+\delta_R$ with $\delta_L\equiv l_L/\epsilon_L$, $\delta_M\equiv l/\epsilon_M$, $\delta_R\equiv l_R/\epsilon_R$, which, in turn, depend on the electrode-terminal site distances l_L and l_R as well as on the intersite distances l [$\epsilon_{L(R)}$ and ϵ_M are the permittivities of the medium surrounding the electrodes and the molecular wire, respectively,[59,60] cf. also Fig. 1(a)]. The energy gaps, Eq. (31), determine the following relation between the site-to-site hopping rate constants:

$$\alpha_0=\beta_0\exp(-\Delta E_1/k_BT),$$
$$\beta_N=\alpha_N\exp(-\Delta E_N/k_BT), \tag{32}$$
$$\beta=\alpha\exp(-\Delta E_M/k_BT).$$

According to the chosen Condon approximation, each site-to-site rate takes the form $k_{mn}=(2\pi/\hbar)|V_{mn}|^2(\mathrm{FC})_{mn}$, where V_{mn} is the electronic transfer matrix element that couples the sites m and n while $(\mathrm{FC})_{mn}$ is the nuclear Franck-Condon factor for the $m\to n$ electronic transition.[61,62] We next suppose that for each electronic transition $m\to n$, only a single vibrational coordinate with frequency $\omega^{(mn)}$ is involved. Thus, one can employ the expression due to Jortner for the Franck-Condon factor,[63] i.e.,

$$(\mathrm{FC})_{mn}=\frac{1}{\hbar\omega^{(mn)}}\Phi_{mn},$$
$$\Phi_{mn}=\exp\left[-S_{mn}\coth\frac{\hbar\omega^{(mn)}}{k_BT}\right]\left(\frac{1+n(\omega^{(mn)})}{n(\omega^{(mn)})}\right)^{\nu_{mn}/2} \times I_{|\nu_{mn}|}(2S_{mn}[n(\omega^{(mn)})(1+n(\omega^{(mn)}))]^{1/2}). \tag{33}$$

Here, $I_\nu(z)$ denotes the modified Bessel function, $n(\omega)=[\exp(\hbar\omega/k_BT)-1]^{-1}$ is the Bose distribution function, and we introduced $S_{mn}\equiv\lambda_{mn}/\hbar\omega^{(mn)}$, with λ_{mn} being the reorganization energy of the $m\to n$ transition and $\nu_{mn}\equiv(E_m-E_n)/\hbar\omega^{(mn)}$.

We now present an analytic expression for the forward rates. Note also that the backward rates are connected with the forward rates by the relations (32). The forward site-to-site rate constants read

$$\alpha_r = \frac{2\pi}{\hbar\omega_r}|V_r|^2\Phi_{\nu_r} \quad (r=0,N), \tag{34}$$

$$\alpha = \frac{2\pi}{\hbar\omega_B}|V_B|^2\Phi_{\nu_B}. \tag{35}$$

For the regular molecular wire under consideration, we have employed the following abbreviations: $\omega^{(nn+1)} \equiv \omega_B$, $\lambda_{nn+1} \equiv \lambda_B$, $V_{nn+1} \equiv V_B$, $\Phi_{nn+1} \equiv \Phi_{\nu_B}$, $\nu_B = (E_n - E_{n+1})/\hbar\omega_B$, $(n=1,2,\ldots N-1)$, $\omega^{(01)} \equiv \omega_0$, $\lambda_{01} \equiv \lambda_0$, $V_{01} \equiv V_0$, $\Phi_{01} \equiv \Phi_{\nu_0}$, $\nu_0 = (E_0 - E_1)/\hbar\omega_0$, $\omega^{(NN+1)} \equiv \omega_{N+1}$, $\lambda_{NN+1} \equiv \lambda_{N+1}$, $V_{NN+1} \equiv V_{N+1}$, $\Phi_{NN+1} \equiv \Phi_{\nu_N}$, $\nu_N = (E_N - E_{N+1})/\hbar\omega_N$, and $\omega^{(0N+1)} \equiv \tilde{\omega}$, $\lambda_{0N+1} \equiv \tilde{\lambda}$, $\Phi_{0N+1} \equiv \tilde{\Phi}_{\nu_+}$, $\Phi_{N+10} \equiv \tilde{\Phi}_{\nu_-}$, $\nu_+ = \Delta E/\hbar\tilde{\omega}$, and $\nu_- = -\Delta E/\hbar\tilde{\omega}$. Electronic couplings between the neighboring sites are shown in Fig. 1(b). The superexchange rate constants are defined by the expressions

$$k_{1(2)}^{(\mathrm{sup})} = \frac{2\pi}{\hbar\tilde{\omega}}|V_{0N+1}(V)|^2\tilde{\Phi}_{\nu_{+(-)}}, \tag{36}$$

where $\tilde{\Phi}_{\nu_+} \equiv \Phi_{0N+1}$, $\tilde{\Phi}_{\nu_-} \equiv \Phi_{N+10}$, $\tilde{\omega} \equiv \omega^{(0N+1)}$, $\tilde{\lambda} \equiv \lambda_{0N+1}$, $\nu_+ = \Delta E/\hbar\tilde{\omega}$, $\nu_- = -\Delta E/\hbar\tilde{\omega}$, and

$$\Delta E = E_0 - E_{N+1} = \Delta E(0) + eV(1 - \eta_L - \eta_R) \tag{37}$$

is the driving force of the ET between the terminal sites. $\Delta E(0) \equiv E_0(0) - E_{N+1}(0)$ is the unbiased driving force. The meaning of the energy gap ΔE, as well as the gaps introduced so far, follows from the scheme of Fig. 3. The square of the transition matrix element between the spatially separated terminal sites reads

$$|V_{0N+1}(V)|^2 = \frac{|V_0 V_B^{N-1} V_{N+1}|^2}{\Pi_{m=1}^{N}\Delta E_{m0}\Delta E_{mN+1}}. \tag{38}$$

This matrix element depends on the voltage bias V via the energy gaps

$$\begin{aligned} \Delta E_{m0} &= E_m - E_0 = \Delta E_1(0) - eV\eta_M m, \\ \Delta E_{mN+1} &= E_m - E_{N+1} = \Delta E_N(0) + eV\eta_M(N-m+1). \end{aligned} \tag{39}$$

In order to derive a more compact expression, we use the scheme in Ref. 64 to obtain

$$|V_{0N+1}(V)|^2 = |V_{0N+1}(0)|^2 e^{\Lambda(V)}, \tag{40}$$

where

$$\Lambda(V) = (eV\eta_M/2)[(1/\Delta E_1(0)) - (1/\Delta E_N(0))]N(N+1). \tag{41}$$

The quantity

$$\begin{aligned} |V_{0N+1}(0)|^2 &\equiv \frac{|V_0 V_{N+1}|^2}{\Delta E_1(0)\Delta E_N(0)} e^{-\zeta(N-1)} \\ [\zeta &= 2\ln(\sqrt{\Delta E_1(0)\Delta E_N(0)}/|V_B|)] \end{aligned} \tag{42}$$

denotes the square of the superexchange matrix element at the absence of an applied voltage.

III. RESULTS AND DISCUSSION

In order to analyze the I-V characteristics let us first note that at room temperature ($k_BT \approx 0.025$ eV) the Fermi distribution function [Eq. (28)] can be replaced by a unit-step function. Therefore, in the voltage region $V>0$, one obtains $\chi_R \simeq 0$. Analogously, one can set $\chi_L \simeq 0$ if $V<0$. Bearing in mind these valid approximations and using the relations between the rate constants, Eq. (32), after introducing the wire populations, Eq. (21), in the expressions (23) and (24), we arrive at the following expression for the stationary current:

$$\begin{aligned} I = I_0 2\pi\hbar(1 - e^{-e|V|/k_BT}) \\ \times\left[\frac{\chi_L K_1 \chi_{-R}}{D_+}\theta(V) - \frac{\chi_R K_2 \chi_{-L}}{D_-}(1-\theta(V))\right]. \end{aligned} \tag{43}$$

Here, $\theta(V)$ is the unit-step function and

$$\begin{aligned} D_+ &= \chi_{-L}(\chi_{-R} + K_2) + 2\chi_L(\chi_{-R} + K_1 + K_2) + \chi_{-R}K_2, \\ D_- &= \chi_{-R}(\chi_{-L} + K_1) + 2\chi_R(\chi_{-L} + K_1 + K_2) + \chi_{-L}K_2. \end{aligned} \tag{44}$$

These analytic expressions allow us to analyze different regimes of charge transmission through the wire, including the sequential and the superexchange pathways.

In what follows, we concentrate on the emergence of interesting rectification effects. In the case under consideration, a molecular wire [composed by a linear arrangement of $N+2$ sites including N internal identical sites, Fig. 1(a)] transmits the electrons in such a manner that its terminal units may be considered as donor and acceptor transmitters, whereas its internal sites act as a regular bridging structure. The internal sites generate a superexchange coupling between the terminal sites, but these sites are also responsible for the sequential (hopping) transfer through the wire. Before presenting a detailed analysis of the results, let us point out that the function (28) exhibits a sudden rise at the resonant voltages $V = V_L^{(\mathrm{res})}$ and $V = -V_R^{(\mathrm{res})}$, where

$$V_L^{(\mathrm{res})} = \Delta E_L(0)/e\eta_L, \tag{45}$$

and

$$V_R^{(\mathrm{res})} = \Delta E_R(0)/e\eta_R. \tag{46}$$

The expressions for $V_L^{(\mathrm{res})}$ and $V_R^{(\mathrm{res})}$ follow from the conditions $\Delta E_L = 0$ and $\Delta E_R = 0$ at $V>0$ and $V<0$, respectively. Because in the regions $0 \leqslant V < V_L^{(\mathrm{res})}$ and $0 > V \geqslant -V_R^{(\mathrm{res})}$ the current through the molecule stays at a rather small value, we concentrate on the mechanisms of current formation in the regions $V \geqslant V_L^{(\mathrm{res})}$ and $V \leqslant -V_R^{(\mathrm{res})}$. To this end, let us note that at strong differences between the overall hopping rates K_1, K_2, and the contact transfer rates χ_s, χ_{-s} charge transmission in the L-MW-R system is limited by the slowest hopping process. We now analyze two distinct possible limiting situations.

A. Weak coupling to the electrodes: Small rectification limit

Let the coupling of the terminal sites to the respective electrodes be weak, so that the overall transfer rates strongly exceed the contact transfer rates. Note that the maximal val-

ues of the contact rates $\chi_{L(R)}$ and $\chi_{-L(-R)}$ coincide with $\Gamma_{L(R)}/\hbar$. This would be the case for a small nuclear rearrangement upon recharging. Thus, to understand the physics of current formation at weak electrode-wire coupling, it suffices to consider the electron transmission with contact transfer rates defined by Eq. (30). Besides, one has to suppose the validity of the inequality

$$K_1, K_2 \gg (\Gamma_L/\hbar), (\Gamma_R/\hbar). \tag{47}$$

As a rule, the unbiased gaps $\Delta E_L(0)$ and $\Delta E_R(0)$ strongly exceed the thermal energy k_BT. Therefore, independent on the precise form of the contact rates, one can set $\chi_{-L} \approx 0$ and $\chi_R \approx 0$ if $V \geqslant V_L^{(\mathrm{res})}$, and $\chi_{-R} \approx 0$ and $\chi_L \approx 0$ if $V \leqslant -V_R^{(\mathrm{res})}$. Noting this circumstance and using the inequalities (47) one reduces the general expression for the current, Eq. (43), to the following simple form [a case of identical terminal sites is considered, i.e., $\Delta E(0)=0$, Eq. (37)]:

$$I \simeq \theta(V - V_L^{(\mathrm{res})}) I_+^{(\mathrm{plat})} + \theta(-V - V_R^{(\mathrm{res})}) I_-^{(\mathrm{plat})}. \tag{48}$$

The two nonzero (plateau) currents read

$$I_+^{(\mathrm{plat})} = I_0 2\pi \frac{\Gamma_L \Gamma_R}{2\Gamma_L + \Gamma_R} \tag{49}$$

and

$$I_-^{(\mathrm{plat})} = -I_0 2\pi \frac{\Gamma_L \Gamma_R}{\Gamma_L + 2\Gamma_R}. \tag{50}$$

Hereafter, we replace the factor $(1-\exp(-e|V|/k_BT))$ by 1. It follows from the fact that, in the given voltage regions, the pronounced inequality $\exp(-e|V|/k_BT) \ll 1$ is fulfilled. The factor only differs from 1 at small voltages, i.e., less than 0.1 V. The rectification ratio for the plateau currents, $\mathrm{RR}^{(\mathrm{plat})} = |I_+^{(\mathrm{plat})}/I_-^{(\mathrm{plat})}|$, thus reads

$$\mathrm{RR}^{(\mathrm{plat})} = \frac{\Gamma_L + 2\Gamma_R}{2\Gamma_L + \Gamma_R}. \tag{51}$$

The maximal rectification is achieved at a large difference between the corresponding width parameters. The effect is not significant, however. For instance, if $\Gamma_R \gg \Gamma_L$ then $\mathrm{RR}^{(\mathrm{plat})}=2$. Note also the different population of the molecular wire by the transferred electrons at $\Gamma_R \gg \Gamma_L$. It follows from Eq. (21) that in this case $\mathcal{P}_{\mathrm{empty}} \approx 1$, $\mathcal{P}_0 \ll 1$, and $\mathcal{P}_{N+1} \ll 1$ if $V \geqslant V_L^{(\mathrm{res})}$, whereas $\mathcal{P}_{\mathrm{empty}} \ll 1$, $\mathcal{P}_0 \approx (1/2)[K_2/(K_1+K_2)]$, and $\mathcal{P}_{N+1} \approx (1/2)[K_1/(K_1+K_2)]$, if $V \leqslant -V_R^{(\mathrm{res})}$. Thus, at a given relation between the contact transfer rates, the wire remains empty (at $V>0$) or captures a single extra electron with probability $\Sigma_\sigma[\mathcal{P}_{0\sigma}+\mathcal{P}_{N+1\sigma}]=2(\mathcal{P}_0+\mathcal{P}_{N+1}) \approx 1$ (at $V<0$). The expressions (49) and (50) are written for a simple form of contact transfer rates, Eq. (30). In a more general case, one has to utilize the expression defined in Eq. (26). The resulting form of the positive current follows from Eq. (49) if one replaces Γ_L by $\Gamma_L F_L$ and Γ_R by $\Gamma_R F_R \exp(\Delta E_R/k_BT)$. If $V<0$, one has to replace the Γ_R and Γ_L in Eq. (50) by $\Gamma_R F_R$ and $\Gamma_L F_L \exp(\Delta E_L/k_BT)$, respectively. Such a substitution only leads to a more smooth transition to the plateau current, both fixed at $V \geqslant V_L^{(\mathrm{res})}$ and $V \leqslant -V_R^{(\mathrm{res})}$. It does not significantly change, however, the rectification ratio for the plateau currents.

B. Strong coupling to the electrodes: Differential negative resistance and pronounced rectification

Let us next consider the transmission regime at a strong coupling of the terminal sites to respective electrodes. In contrast to the inequalities, Eq. (47), we now suppose that

$$K_1, K_2 \ll (\chi_L + \chi_{-L}), (\chi_R + \chi_{-R}). \tag{52}$$

The general current expressions, Eqs. (23) and (24), assume the form

$$I = I_{\mathrm{sup}}(V) + I_{\mathrm{seq}}(V), \tag{53}$$

where the superexchange current component reads

$$I_{\mathrm{sup}}(V) \simeq I_0 2\pi\hbar \left[\theta(V) \frac{\chi_L k_1^{(\mathrm{sup})}}{\chi_{-L} + 2\chi_L} - \theta(-V) \frac{\chi_R k_2^{(\mathrm{sup})}}{\chi_{-R} + 2\chi_R} \right]. \tag{54}$$

It describes a single step distant jumps between the terminal wire units. The sequential component of the total current takes a completely different form, namely,

$$I_{\mathrm{seq}}(V) \simeq I_0 2\pi\hbar \left[\theta(V) \frac{\chi_L}{\chi_{-L} + 2\chi_L} \frac{\alpha_0 \alpha_N}{\beta_0 + \alpha_N} \times \left[1 + \xi_+ \frac{1 - \gamma_+^{N-1}}{1 - \gamma_+} \right]^{-1} - \theta(-V) \frac{\chi_R}{\chi_{-R} + 2\chi_R} \frac{\beta_0 \beta_N}{\beta_0 + \alpha_N} \times \left[1 + \xi_- \frac{1 - \gamma_-^{N-1}}{1 - \gamma_-} \right]^{-1} \right]. \tag{55}$$

The parameters

$$\xi_+ = \frac{1 - (\alpha/\alpha_N)(1 - \gamma_+)}{(\alpha/\beta_0) + (\alpha/\alpha_N)}, \quad \xi_- = \frac{1 - (\beta/\beta_0)(1 - \gamma_-)}{(\beta/\alpha_N) + (\beta/\beta_0)} \tag{56}$$

specify the dependence of the sequential current component on the wire length. Different dependencies of the superexchange and sequential current components on the wire length allow one to specify the type of charge transmission through a concrete molecular wire. Note also that a definite discrimination of the current components only becomes possible if the inequalities (14) and (52) are fulfilled in the course of charge transmission. They characterize such a type of transmission where the hopping processes between a terminal wire unit and the opposite electrode are much faster than the escape of an electron from the same terminal unit to other wire units [see the scheme in Fig. 2(a)].

1. Symmetric case

The contribution related to the sequential and the superexchange pathway strongly depends on the relation between the parameters defining all hopping rates. Figure 4 depicts the respective current versus the length of the wire. The chosen transmission regime corresponds to the symmetric case where $\eta_L = \eta_R$, $\Delta E_L(0) = \Delta E_R(0)$, $\Delta E_1(0) = \Delta E_N(0)$, and $\Delta E(0)=0$ [cf. Eqs. (29)–(37)]. It can be deduced from Fig. 4 that at a given set of parameters, the superexchange pathway dominates the current formation for short molecular wires.

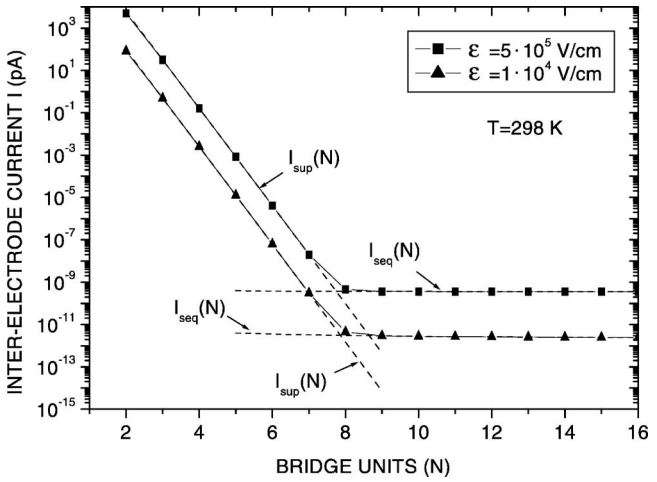

FIG. 4. Length dependence of the current through a regular molecular wire. At the given set of parameters, the superexchange mechanism of the current formation dominates for a short molecular wire (up to six internal units), while the thermally activated sequential mechanism exceeds the superexchange for longer wires [calculations according to Eqs. (43) and (44)]. The completely symmetric case has been considered using the following parameters: $\delta_L=\delta_R=4$ Å, $\delta_M=3$ Å, $\omega_0=\omega_N=\omega_B=\tilde{\omega}=500\ \mathrm{cm}^{-1}$, $V_0=V_N=0.1$ eV, $V_B=0.05$ eV, $\Delta E_L(0)=\Delta E_R(0)=0.2$ eV, $\Delta E_1(0)=\Delta E_N(0)=0.6$ eV, $\Delta E(0)=0$, $\lambda_0=\lambda_{N+1}=1.2$ eV, $\lambda_B=0.5$ eV, $\tilde{\lambda}=0.2$ eV, and $\Gamma_L=\Gamma_R=0.1$ eV.

Noting this fact, we next analyze the *I-V* characteristics for a short molecular wire.[38,41,50] Additionally, we discuss the voltage dependence of the wire conductance, i.e., the nonlinear differential conductivity,

$$g(V)=dI(V)/dV. \tag{57}$$

Figure 5(a) depicts the nonlinear *I-V* characteristics [in the symmetric case and at $n(\tilde{\omega})\ll 1$]. According to the symmetry relation $I(V)=-I(-V)$, we only concentrate on the regime $V>0$. As a main observation we notice that the current reaches a maximum at a finite voltage, and afterward drops down to zero. Consequently, the differential conductance covers regions with a *negative differential resistance* [see Fig. 5(b)].

In order to explain this intriguing behavior we take into consideration that in the case $n(\tilde{\omega})\ll 1$ the Bessel function entering the current formula [cf. Eqs. (33)–(53)] can be approximated by its asymptotic form $I_\nu(z)\approx(z/2)^\nu/\Gamma(\nu+1)$ (Ref. 65) where $\Gamma(x)$ is the Gamma function. Thus, Eq. (36) takes the form

$$\tilde{\Phi}_\nu \approx \left[\frac{1+n(\tilde{\omega})}{n(\tilde{\omega})}\right]^{\nu/2}[n(\tilde{\omega})(1+n(\tilde{\omega}))]^{|\nu|/2}\frac{\tilde{S}^{|\nu|}}{\Gamma(|\nu|+1)}e^{-\tilde{S}}, \tag{58}$$

with $\tilde{S}=\tilde{\lambda}/\hbar\tilde{\omega}$. If ν is positive, then the product $[(1+n(\tilde{\omega}))/n(\tilde{\omega})]^{\nu/2}[n(\tilde{\omega})(1+n(\tilde{\omega}))]^{|\nu|/2}$ reduces to $(1+n(\tilde{\omega}))^\nu$. For a negative ν the product equals $n(\tilde{\omega})^{|\nu|}$. Since charge transmission is considered for the case $n(\tilde{\omega})\ll 1$, only those superexchange transfer processes where $\nu\geqslant 0$ contribute. Therefore, we may use $\tilde{\Phi}_\nu$ in the following approximate form:

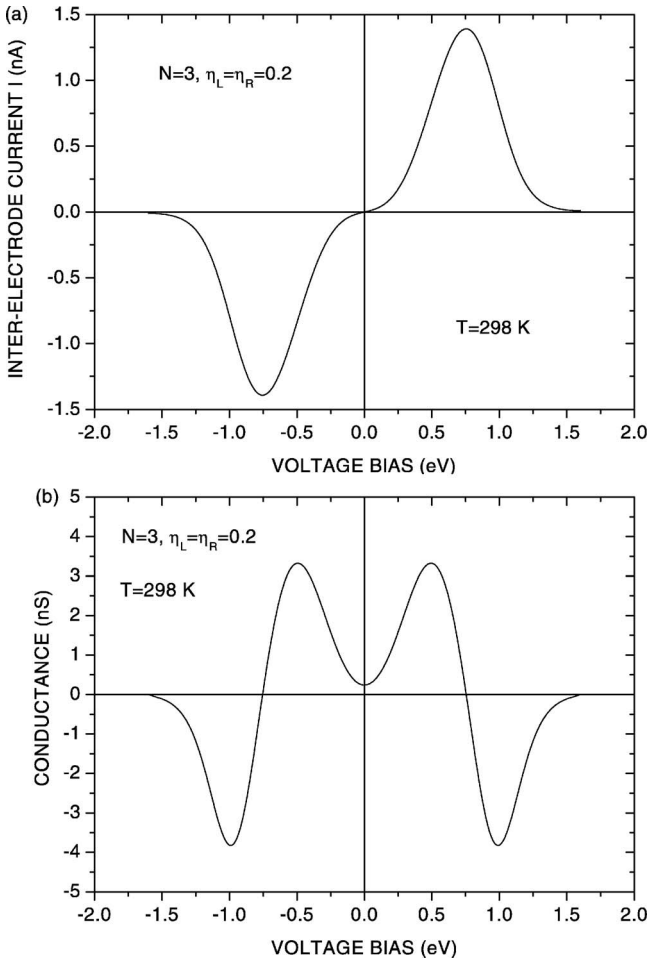

FIG. 5. Current-voltage (panel a) and conductance-voltage (panel b) characteristics of a regular molecular wire with three internal units. The used parameters are identical with those of Fig. 4 which correspond to the completely symmetric situation. The current suppression and, correspondingly, the appearance of a *negative differential resistance* is caused by multiphonon processes.

$$\tilde{\Phi}_\nu \approx e^{-\tilde{S}}\tilde{S}^\nu/\Gamma(\nu+1) \quad (\nu\geqslant 0). \tag{59}$$

According to its definition, the parameter ν coincides with the number of vibrational quanta necessary to bypass the energy gap between the levels of the terminal wire units. In the case of the $0\rightarrow N+1$ transfer, this gap equals ΔE. The backward transfer $N+1\rightarrow 0$ is characterized by the gap $-\Delta E$. Thus, if the superexchange transition is accompanied by high-frequency vibrational quanta, it only occurs at a positive driving forces $\Delta G=\Delta E$ and $\Delta G=-\Delta E$, being associated with the forward and backward electron transfer reactions, respectively.

In the symmetric situation under discussion, the parameter $\nu=\Delta E/\hbar\tilde{\omega}$ is given by the expression

$$\nu = eV(1-\eta_L-\eta_R)/\hbar\tilde{\omega}, \tag{60}$$

which is positive for $V>0$. Therefore, in virtue of Eqs. (30), (33), (36), (54), and (59), the current through the molecular wire is described by a rather simple expression, reading

$$I \approx I_{\mathrm{sup}} \approx I_0 2\pi\hbar \frac{n_F(\Delta E_L)}{1+n_F(\Delta E_L)} k_1^{(\mathrm{sup})} \quad (V \geqslant 0), \tag{61}$$

with

$$k_1^{(\mathrm{sup})} \approx \frac{2\pi}{\hbar^2 \tilde{\omega}} |V_{0N+1}(0)|^2 \frac{\tilde{S}^{\nu}}{\Gamma(\nu+1)} e^{-\tilde{S}}. \tag{62}$$

To obtain the expression (61) we used the identity $\chi_{L(R)}/[\chi_{-L(-R)}+2\chi_{L(R)}]=[\exp(\Delta E_{L(R)}/k_BT)+2]^{-1}$ $=n_F(\Delta E_{L(R)})/[1+n_F(\Delta E_{L(R)})]$, being valid for any form of contact transfer rates $\chi_{L(R)}$ and $\chi_{-L(-R)}$.

In line with Eqs. (60)–(62), the voltage dependence of the current is defined by the distribution function $n_F(\Delta E_L)$ and the parameter ν. Note also that in the symmetric case one obtains $\Lambda(V)=0$, so that $|V_{0N+1}(V)|^2=|V_{0N+1}(0)|^2$, cf. Eq. (40). At positive voltages, the energy gap ΔE_L, Eq. (29), decreases with the increase of V. It vanishes at the resonant voltage [Eq. (45)] and it becomes negative at $V>V_L^{(\mathrm{res})}$. Therefore, the function $n_F(\Delta E_L)$ increases only in the region $0 \leqslant V \leqslant V_L^{(\mathrm{res})}$. If $V>V_L^{(\mathrm{res})}$, however, this function does not change, i.e., now $n_F(\Delta E_L) \simeq 1$. Thus, the decrease of the current (and the appearance of a negative differential resistance) is related to the decrease of the superexchange rate $k_1^{(\mathrm{sup})}$. A detailed inspection of the function, Eq. (59), shows that it exhibits a strong decrease at large ν. As far as the quantity ΔE, Eq. (37), increases with an increase of V, the number of vibrational quanta ν compensating this increase increases as well. Therefore, this effect explains the drop of the current in the voltage region $V>V_L^{(\mathrm{res})}$. At negative voltages, the resonant electron transition starts at $V=-V_R^{(\mathrm{res})}$, where $V_R^{(\mathrm{res})}$ is defined by Eq. (46). In a symmetric case, the resonant voltages $V_R^{(\mathrm{res})}$ and $V_L^{(\mathrm{res})}$ coincide. Thus, the I-V characteristics is inversion symmetric and the conductance-voltage characteristics is reflection symmetric in this case as a function of applied voltage bias V.

2. Asymmetric case

The discussed symmetric behavior is changed if the resonant voltages at $V>0$ and $V<0$ do not coincide. It follows from Eqs. (45) and (46) that an asymmetry appears if either $\eta_R \neq \eta_L$, i.e., the terminal sites are positioned differently with respect to the electrode, or if $\Delta E_R(0) \neq \Delta E_L(0)$, i.e., the energy gaps between each terminal site level and the respective Fermi energy are different. Likewise, an asymmetry appears if, simultaneously, $\eta_R \neq \eta_L$ and $\Delta E_R(0) \neq \Delta E_L(0)$. Figure 6 depicts the asymmetric I-V characteristics for the particular case $\eta_R \neq \eta_L$ and $E_R(0)=\Delta E_L(0)$. Generally, if $\eta_R \neq \eta_L$, the coupling of the terminal wire units to the opposite electrodes is also varied, resulting in $\Gamma_R \neq \Gamma_L$. However, if the inequalities (47) are valid and, thus, the limiting part of the transmission process is given by a distant electron hopping between the terminal wire units, the relation between the width parameters Γ_R and Γ_L becomes unimportant.

The superexchange mechanism of an asymmetric current formation becomes more complex if $E_0(0) \neq E_{N+1}(0)$. In this case, a nonzero gap $\Delta E(0)>0$ exists even at $V=0$. This means that $\Delta E_N(0)=\Delta E_1(0)+\Delta E(0)$ and $\Delta E_R(0)=\Delta E_L(0)$ $-\Delta E(0)$. Because $\Delta E_1(0) \neq \Delta E_N(0)$ the quantity $\Lambda(V)$, Eq. (41), does not vanish, yielding for the current the result

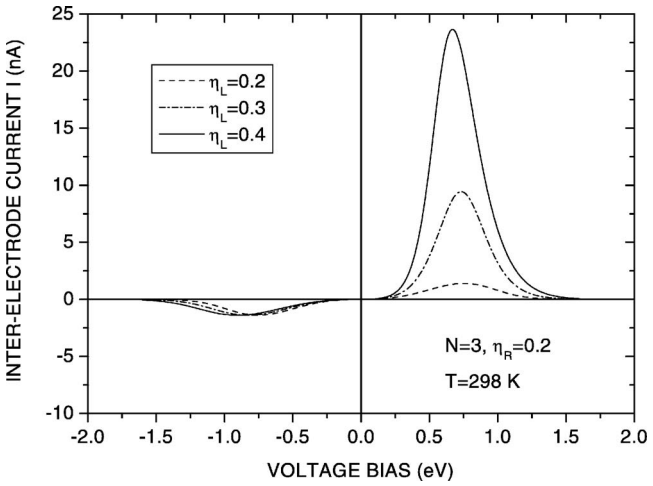

FIG. 6. Asymmetric I-V characteristics of a regular molecular wire with three internal units. The used parameters are identical with those of Fig. 4 except that $\Gamma_L=0.1$ eV and $\Gamma_R=0.2$ eV. The asymmetry results from the difference between the edge voltage division factors η_L and η_R.

$$I \approx I_0 \frac{4\pi^2}{\hbar\tilde{\omega}} |V_{0N+1}(0)|^2 \frac{n_F(\Delta E_L)}{1+n_F(\Delta E_L)} \tilde{\Phi}_{\nu_+} e^{\Lambda(V)} \quad (V>0), \tag{63}$$

where the function $\tilde{\Phi}_{\nu_+}$ is given by Eq. (59) with

$$\nu = \nu_+ = [\Delta E(0) + eV(1-\eta_L-\eta_R)]/\hbar\tilde{\omega}. \tag{64}$$

In Eq. (63), the quantity $\Lambda(V)$, Eq. (41), adds an additional voltage dependence, which is caused by the energetic asymmetry of the terminal wire groups. As far as $\nu_+ \geqslant 0$ and depending on the value of the energy gap $\Delta E(0)$ (at $V=0$), the distant superexchange electron transition is accompanied by a large number of vibrational quanta even at a small applied voltage. This leads to the suppression of the current in the region $V>0$, especially at $V \geqslant V_L^{(\mathrm{res})}$. The suppression is diminished by the factor $\exp(\Lambda(V))$, which increases at a positive voltage. This behavior is dictated by the condition $\Lambda(V)>0$ valid at $\Delta E(0)>0$. Nevertheless, at positive voltages, the electron transmission accompanied by a multiphonon compensation of the energy gap $\Delta E=\Delta E(0)$ $+eV(1-\eta_L-\eta_R)$ represents an important mechanism of current suppression.

Yet another situation occurs at $V<0$. Now, the driving force $\Delta G=-\Delta E$ of the $0 \leftarrow N+1$ transition is positive only at $V<-V^*$, where the critical voltage

$$V^* = \Delta E(0)/e(1-\eta_L-\eta_R) \tag{65}$$

is defined by the condition $\Delta G=0$. Thus, in accordance with expression (59) electron transmission through the wire becomes effective only when $V<-V^*$. In this case, the parameter

$$\nu = \nu_- = [-\Delta E(0) + e|V|(1-\eta_L-\eta_R)]/\hbar\tilde{\omega} \tag{66}$$

becomes positive. The current then takes the form

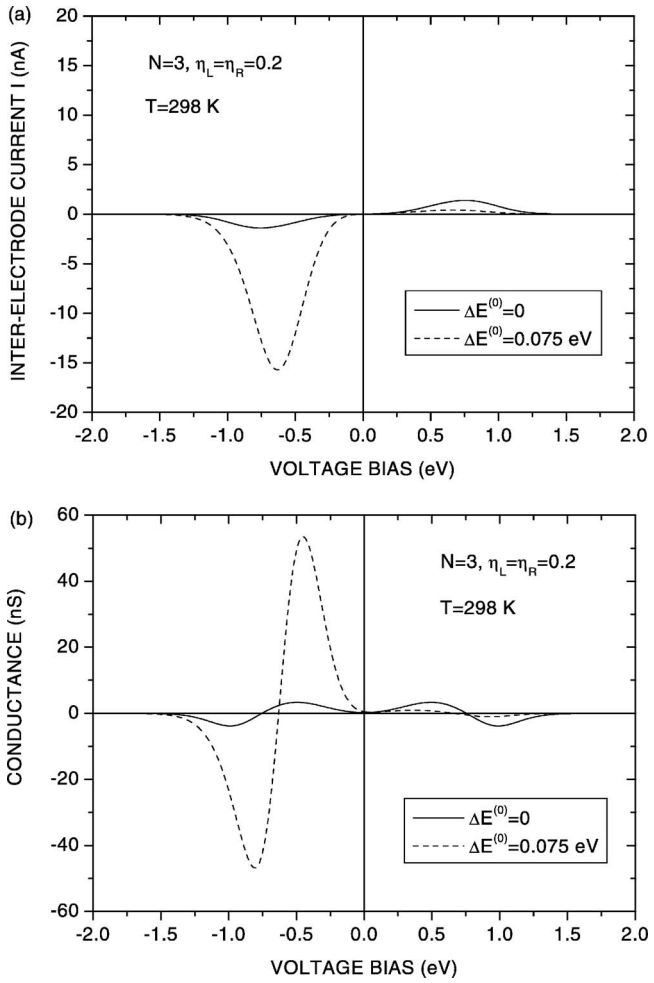

FIG. 7. Asymmetric *I-V* (panel a) and differential conductance-voltage (panel b) characteristics of a linear regular molecular wire consisting of three internal units. The asymmetry appears at a nonzero value of the unbiased driving force $\Delta E(0)$ corresponding to the distant superexchange electron transfer between the terminal wire units. It results in different multiphonon processes at $V>0$ and $V<0$. The parameters are the same as those used in Fig. 4, except that $\Delta E(0)=0.025$ eV, $\Gamma_L=0.1$ eV, and $\Gamma_R=0.2$ eV. In this case, we set $\Delta E_R(0)=\Delta E_L(0)-\Delta E(0)$ and $\Delta E_N(0)=\Delta E_1(0)+\Delta E(0)$.

$$I \approx I_0 \frac{4\pi^2}{\hbar\tilde{\omega}} |V_{0N+1}(0)|^2 \frac{n_F(\Delta E_R)}{1+n_F(\Delta E_R)} \tilde{\Phi}_{\nu_-} e^{-\Lambda(|V|)}, \quad V<-V^*. \tag{67}$$

The essential difference between the *I-V* characteristics at $V<0$ and at $V>0$ is related to the energy gaps ΔE_L and ΔE_R, as well as to the parameters ν_+ and ν_-. Because $\Delta E_R < \Delta E_L$, the function $n_F(\Delta E_R)$ increases faster than how much the function $n_F(\Delta E_L)$ decreases. Bearing in mind that a larger value for ν_+ is reached as compared to ν_- at smaller voltages, the suppression of the current at $V>0$ occurs also at smaller voltages, as compared to the suppression of the current at $V<0$. It emerges then a distinct current rectification, being clearly depicted with Fig. 7.

It follows from Eq. (21) that at strong wire-electrode couplings, the wire populations are $\mathcal{P}_{\text{empty}} \ll 1$, $\mathcal{P}_{0\uparrow}+\mathcal{P}_{0\downarrow}=2\mathcal{P}_0 \approx 1$, and $\mathcal{P}_{N+1} \ll 1$ if $V \geqslant V_L^{(\text{res})}$, whereas $\mathcal{P}_{\text{empty}} \ll 1$, $\mathcal{P}_0 \ll 1$, and $\mathcal{P}_{N+1\uparrow}+\mathcal{P}_{N+1\downarrow}=2\mathcal{P}_{N+1} \approx 1$ if $V \geqslant -V_L^{(\text{res})}$. One notices a different character of this population in comparison to the case of a weak coupling to the electrodes. In particular, at a strong coupling (when the width parameters Γ_L and Γ_R are large) a molecular wire traps a single extra (transferred) electron either by the left or by the right terminal site. Such trapping does not depend on the value of the width parameters but exclusively on the current direction. At the same time, at a weak coupling to the electrodes (when the width parameters Γ_L and Γ_R are small), the wire can remain empty if the coupling to one of the electrodes strongly exceeds the coupling to the other electrode.

IV. CONCLUSIONS

With the present work we discussed the current-voltage (*I-V*) characteristics of a molecular wire attached to two nanoelectrodes. Our focus was on the influence of terminal wire groups on the current formation. The model description for the wire assumes that the internal molecular sites act as bridging groups. Therefore, they cause a superexchange electronic coupling between the terminal sites but, in addition, they also form a sequential electron pathway among these sites. We presented detailed studies of the *I-V* and conductance-voltage characteristics for the two limiting cases of (i) a weak and (ii) a strong molecular wire-electrode coupling. In the case of a weak coupling, the width parameters Γ_L and Γ_R are small so that the kinetics of charge transmission are characterized by the condition (47). A limiting stage of this kinetics is associated with charge hopping between the terminal wire units and the adjacent electrodes. A rectification effect only appears at a large difference between the width parameters. But, the effect is not substantial, see Eq. (51), at $\Gamma_R \gg \Gamma_L$ or $\Gamma_L \gg \Gamma_R$. A completely different situation occurs at strong wire-electrode couplings: The coupling to vibrational modes results in a distinct peak in the *I-V* characteristics which is followed by current suppression. Thus, a *negative differential resistance* behavior occurs. This intriguing current suppression is caused by multiphonon processes which accompany the single step superexchange electron transition between the terminal wire units. These multiphonon processes also become responsible for a pronounced rectification effect (note the dotted lines in Fig. 7).

In the most simple situation, the multiphonon rectification can be observed in a system of a left electrode, a molecular wire, and a right electrode, where the electrodes are identical and where the energetic positions of the terminal groups with respect to the opposite electrodes coincide. It is then only necessary to create a small structural perturbation near one of the identical terminal groups in order to form the unbiased energy gap $\Delta E(0) \neq 0$ between the electronic levels of these groups, see Eq. (37). This multiphonon rectification effect is caused by vibrational relaxations within the terminal groups of the system. Rectification may be also related to the voltage division factors η_L and η_R that define the level shift of the terminal groups (see Fig. 6). The rectification feature of the molecular wire, as depicted in the Figs. 6 and 7, is exclusively connected with the superexchange mechanism of a single step electron transfer between the terminal wire sites. Such a description is based on the observation that the superexchange transfer may represent the limiting step of the

transmission process in the whole system. This would be the case if the following two conditions are fulfilled: (i) it is necessary that the electron transfer between the electrodes and the respective terminal wire units is much faster than both, the direct transfer between the terminal units and, as well as the transfer between each terminal unit and the neighboring internal wire unit, cf. the kinetic scheme depicted in Fig. 2(a) and the inequality Eq. (14); and (ii) the thermal activated sequential (hopping) transfer between the terminal units has to be less efficient than the superexchange transfer. Figure 4 indicates that this, in fact, can occur during electron transfer through a short molecular wire, provided that $k_1^{(\mathrm{sup})} \gg \alpha_0$ and $k_2^{(\mathrm{sup})} \gg \beta_N$.

Note also the specific charging effect which is related to an asymmetric resonant electron transfer through the wire. At weak wire-electrode couplings [see Eq. (47)], the wire is either free of transferred electrons or it has captured a single extra (transferred) electron by the terminal site which is more weakly coupled to the adjacent electrode. In the considered example ($\Gamma_R \gg \Gamma_L$), it is the left terminal site which is occupied by the transferred electron. This occurs at positive voltages. At the same time, the wire remains empty at negative voltages. If the wire-electrode couplings are strong [see condition (52)] a resonant transmission is accompanied by a trap mechanism for a single transferred electron by the left ($V>0$) or the right ($V<0$) terminal site. This effect can in principle be observed with electron paramagnetic resonance (EPR), or in using optical spectroscopy.

ACKNOWLEDGMENTS

One of us (E.G.P.) gratefully acknowledge the generous support by the Alexander von Humboldt Foundation. This work has also been supported by the NATO-Collaborative Linkage Grant "Theory of Charge Motion through Molecular Wires" (Ya.R.Z.); by the collaborative research centre SFB 450 (V.M.), the collaborative research centre SFB 486 (P.H.), the focus project SPP 1243 "quantum transport on the molecular scale" by the DFG (P.H.), and by the Nanosystems Initiative Munich (NIM) (P.H.).

[1] J. Taylor, M. Brandbyge, and K. Stokbro, Phys. Rev. B **68**, 121101 (2003).
[2] R. Pati and S. P. Karna, Phys. Rev. B **69**, 155419 (2004).
[3] J. Chen and M. A. Reed, Science **286**, 1550 (1999).
[4] C. Krzeminski, C. Delerue, G. Allan, and D. Vuillaume, Phys. Rev. B **64**, 085405 (2001).
[5] R. M. Metzger, T. Xu, and R. J. Peterson, J. Phys. Chem. B **105**, 7280 (2001).
[6] S. Kubatkin, A. Danilov, M. Hjort, J. Cornil, J.-L. Bredas, N. Stuhr-Hansen, P. Hedegard, and T. Bjernholm, Nature (London) **425**, 698 (2003).
[7] J. Lehmann, S. Camalet, S. Kohler, and P. Hänggi, Chem. Phys. Lett. **368**, 282 (2003).
[8] K. Flensberg, Phys. Rev. B **68**, 205323 (2003).
[9] J. Paaske and K. Flensberg, Phys. Rev. Lett. **94**, 176801 (2005).
[10] J. Kong, N. R. Franklin, C. Zhou, M. G. Chaplin, S. Peng, K. Chou, and H. Dai, Science **287**, 622 (2000).
[11] J. Chen and M. A. Reed, Chem. Phys. **281**, 127 (2002).
[12] J. Chen, J. Su, W. Wang, and M. A. Reed, Physica E (Amsterdam) **16**, 17 (2003).
[13] J. Taylor, H. Guo, and J. Wang, Phys. Rev. B **63**, 245407 (2001).
[14] J. Taylor, M. Brandbyge, and K. Stokbro, Phys. Rev. Lett. **89**, 138301 (2002).
[15] H. Bash and M. Ratner, J. Chem. Phys. **120**, 5771 (2004).
[16] M. DiVenrta, S. Pantelides, and N. D. Lang, Phys. Rev. Lett. **84**, 976 (2000).
[17] R. Baer and D. Neuhauser, Int. J. Quantum Chem. **91**, 524 (2002).
[18] H. Chen, J. Q. Lu, J. Wu, R. Note, H. Mizuseki, and Y. Kawazoe, Phys. Rev. B **67**, 113408 (2003).
[19] Y. Xue, S. Datta, and M. A. Ratner, Chem. Phys. **281**, 151 (2002).
[20] P. Dample, A. W. Ghosh, and S. Datta, Chem. Phys. **281**, 171 (2002).
[21] P. Hänggi, M. Ratner, and S. Yaliraki, Chem. Phys. **281**, 111 (2002).
[22] G. Cuniberti, G. Fagas, and K. Richter, Lect. Notes Phys. **680**, 1 (2005).
[23] C. Joachim and M. A. Ratner, Proc. Natl. Acad. Sci. U.S.A. **102**, 8801 (2005).
[24] R. Landauer, Phys. Lett. A **8**, 81 (1981).
[25] M. Büttiker, Phys. Rev. B **33**, 3020 (1986).
[26] M. Cizek, M. Thoss, and W. Domcke, Phys. Rev. B **70**, 125406 (2004); Czech. J. Phys. **55**, 189 (2005).
[27] A. Mitra, I. Aleiner, and A. J. Mills, Phys. Rev. B **69**, 245302 (2004).
[28] J. Lehmann, S. Kohler, V. May, and P. Hänggi, J. Chem. Phys. **121**, 2278 (2004).
[29] E. G. Emberly and G. Kirczenow, Phys. Rev. B **61**, 5740 (2000).
[30] Y.-C. Chen, M. Zwolak, and M. Di Ventra, Nano Lett. **4**, 1709 (2004).
[31] M. Galperin, A. Nitzan, and M. Ratner, Phys. Rev. B **74**, 075326 (2006).
[32] J. Koch, M. Semmelhack, F. von Oppen, and A. Nitzan, Phys. Rev. B **73**, 155306 (2006).
[33] F. J. Kaiser, M. Strass, S. Kohler, and P. Hänggi, Chem. Phys. **322**, 193 (2006).
[34] F. J. Kaiser, P. Hänggi, and S. Kohler, Eur. Phys. J. B **54**, 201 (2006).
[35] C. Benesch, M. Cizek, M. Thoss, and W. Domcke, Chem. Phys. Lett. **430**, 355 (2006).
[36] E. G. Petrov, I. S. Tolokh, A. A. Demidenko, and V. V. Gorbach, Chem. Phys. **193**, 237 (1995).
[37] C. Kergueris, J.-P. Bourgoin, S. Palacin, D. Esteve, C. Urbina, M. Magoga, and C. Joachim, Phys. Rev. B **59**, 12505 (1999).
[38] E. G. Petrov and P. Hänggi, Phys. Rev. Lett. **86**, 2862 (2001).
[39] A. Nitzan, Annu. Rev. Phys. Chem. **52**, 681 (2001).
[40] A. M. Kuznetsov and J. Ulstrup, J. Chem. Phys. **116**, 2149 (2002).
[41] E. G. Petrov, V. May, and P. Hänggi, Chem. Phys. **296**, 251 (2004).
[42] A. Nitzan and M. Ratner, Science **300**, 1384 (2003).
[43] A. Tsoi, M. A. Ratner, and A. Nitzan, J. Chem. Phys. **118**, 6072 (2003).
[44] M. Galperin and A. Nitzan, Ann. N.Y. Acad. Sci. **1006**, 48 (2003).
[45] M. Galperin, M. A. Ratner, and A. Nitzan, J. Chem. Phys. **121**, 11965 (2004).
[46] E. G. Petrov, Ye. V. Shevchenko, V. I. Teslenko, and V. May, J. Chem. Phys. **115**, 7107 (2001).
[47] E. G. Petrov, Ye. V. Shevchenko, and V. May, Chem. Phys. **288**, 269 (2003).
[48] E. G. Petrov, V. I. Teslenko, and V. May, J. Chem. Phys. **121**, 5328 (2004).
[49] V. May and E. G. Petrov, Phys. Status Solidi B **241**, 2168 (2004).
[50] E. G. Petrov, V. May, and P. Hänggi, Chem. Phys. **281**, 211 (2002).
[51] J. Lehmann, G.-L. Ingold, and P. Hänggi, Chem. Phys. **281**, 199 (2002).
[52] E. G. Petrov, V. May, and P. Hänggi, Chem. Phys. **319**, 380 (2005).
[53] E. G. Petrov, Chem. Phys. **326**, 151 (2006).
[54] E. G. Petrov, V. May, and P. Hänggi, Phys. Rev. B **73**, 045408 (2006).
[55] A. Nitzan, J. Phys. Chem. A **105**, 2677 (2001).
[56] N. Zimbovskaya and G. Gumbs, Appl. Phys. Lett. **81**, 1518 (2002).
[57] T. Holstein, Ann. Phys. (N.Y.) **8**, 325 (1959).
[58] Strong conditions at which the overall transfer rate appears as the sum of sequential and superexchange contributions have been derived in Ref. 47.
[59] I. R. Peterson, D. Vuillaume, and R. M. Metzger, J. Phys. Chem. A **105**, 4702 (2001).
[60] E. G. Petrov, Low Temp. Phys. **31**, 338 (2005).
[61] R. A. Marcus and N. Sutin, Biochim. Biophys. Acta **811**, 265 (1985).
[62] U. Weiss, *Quantum Dissipative Systems*, 2nd ed. (World Scientific, Singapore, 1998).
[63] J. Jortner, J. Chem. Phys. **64**, 4860 (1976).
[64] E. G. Petrov, and V. May, J. Chem. Phys. **120**, 4441 (2004).
[65] I. S. Grandshtein and I. M. Ryzhyk, *Tables of Integrals, Series, and Products*, 5th ed. (Academic, San Diego, 1994).